Shake Table Tests on One-Quarter Scale Models of Masonry Houses Retrofitted with PP-Band Mesh

Navaratnarajah Sathiparan,[a] Paola Mayorca,[b] and Kimiro Meguro[c]

This paper introduces a technically feasible and economically affordable retrofitting option for seismically vulnerable masonry structures in developing countries using polypropylene bands (PP-bands). The results of the basic material tests and shake table tests on building models show that the PP-band retrofitting technique can enhance the safety of both existing and new masonry buildings, even during severe ground motions, for instance an earthquake with a Japan Meteorological Agency (JMA) seismic intensity of 7. Therefore, the proposed method is an optimum solution for promoting safer building construction in developing countries and can contribute to earthquake disaster mitigation in the future. [DOI: 10.1193/1.3675357]

INTRODUCTION

More than 60% of people in the world are living in masonry buildings that are made by piling up bricks, sun-dried mud bricks (unburnt brick, generally called adobe), stone, or concrete blocks. Population statistics show that this ratio is rather high, especially in developing countries. Masonry buildings without earthquake reinforcement have claimed scores of victims in all parts of the world. The results of earthquake damage investigations and studies conducted in earthquake-prone regions of the world have revealed that masonry buildings can collapse after just a few seconds of earthquake shaking, thus they are a major cause of human fatalities during earthquakes.

Based on post-earthquake damage surveys, the major types of masonry failure modes have been identified as: (1) out-of-plane wall collapse, (2) separation of adjacent walls, (3) in-plane diagonal cracking, and (4) cracking due to stress concentrations around openings (doors and windows).

Figure 1 shows examples of out-of-plane damage in unreinforced masonry houses. This failure mode is common when the main direction of the seismic motion is perpendicular to the masonry walls and they have insufficient transversal supports. Figure 1a shows examples of structures with flexible roofs. In the first case, the roof is a wooden truss supported on two of the house walls. The other two walls do not have any support at the top and as a result the upper portions collapsed. Figure 1b shows an unreinforced masonry house with a reinforced concrete (RC) roof that is not supported by all of the walls. As a result, the walls that were not restrained by the roof collapsed. Failure of the connections between walls can

[a] Post Doctoral Fellow, Institute of Industrial Science, University of Tokyo, Japan
[b] Senior Engineer, Det Norske Veritas AS, Norway
[c] Professor/Director, ICUS, Institute of Industrial Science, University of Tokyo, Japan

Earthquake Spectra, Volume 28, No. 1, pages 277–299, February 2012;

(a) (b) (c)

Figure 1. Out-of-plane failure: (a and b) collapse of masonry walls, and (c) failure of a wall connection (Mayorca 2001).

also cause out-of-plane failure, as observed in Figure 1c. Generally, the corners of any structure are associated with stress concentrations. If the connection between two walls is weak, for example due to poor-quality workmanship, it can easily fail. As a result, each of the connecting walls becomes an independent structure and is only supported at the bottom, which is a worst-case scenario during an earthquake as out-of-plane failure is very likely to occur under these circumstances.

Masonry walls are relatively stiff and if inertial loads are adequately transferred to them, they act as the main lateral resistance system in a building. During shear deformation the loaded diagonal shortens and the opposite diagonal is subjected to tension. If the load exceeds the wall strength this deformation will cause diagonal cracking parallel to the shortened diagonal. Because earthquake loads are cyclic, the successive action reversal will generate X-type cracking, as shown in Figure 2a. In-plane behavior largely depends on the wall aspect ratio. Openings in the masonry walls will form short piers that will experience concentrations of shear stresses and hence develop diagonal cracks (Figure 2b). At the corners of the openings, tension cracks may appear due to the reverse cyclic stress induced by lateral loading. Until the shear cracks become unduly severe, the gravity-load-carrying capacity of the walls is not jeopardized.

It is clear from reports that in most large-scale earthquake disasters the principal cause of death is the collapse of buildings. The collapse of nonengineered masonry is one of the

(a) (b)

Figure 2. In-plane cracking of unreinforced masonry walls (Meguro et al. 2001).

major causes of human casualties during recent earthquakes in developing countries (Coburn and Spence 2002). Therefore, retrofitting seismically vulnerable masonry structures is a key issue for earthquake disaster mitigation in developing countries. Retrofitting proposals for developing countries should respond to the structural demands of the buildings with regard to their strength and/or deformability, as well as to the availability of low-cost materials, including manufacturing and delivery, the practicability of the proposed construction method, and the cultural acceptability of the retrofitting method in each region (Yoshimura and Meguro 2004). Considering these issues, a technically feasible and economically affordable retrofitting technique utilizing polypropylene bands (PP-bands), which are commonly used for packaging, has been developed and many different aspects have been studied by the Meguro Laboratory at the Institute of Industrial Science, University of Tokyo (Mayorca and Meguro 2004).

Full-scale model tests make it possible to obtain data similar to that of real structures. However, they require large testing facilities and generous research funds, so they are more difficult to execute. Recently, reduced-scale models have become more popular because the overall behavior of a system can be understood from a scale model. Also, the potential of reduced-scale models is not limited to research. Because performing numerous tests does not require significant additional investment, the models can also be used as educational tools to increase public awareness of the vulnerability of masonry houses and the need for retrofitting. Public demonstrations using scale models have been carried out (for instance, in Muzaffarabad, Pakistan after the 2006 Kashmir earthquake and in 2008 in Kathmandu, Nepal) and have had a great impact on the general public, politicians, practitioners, and the mass media. However, these demonstrations used relatively large models, which are expensive and require a great deal of preparation. With reduced-scale models like the ones presented in this paper, it may be possible to expand the scope of these demonstrations, making them more affordable.

The applicability of PP-band mesh for retrofitting unreinforced masonry structures has been tested under static (Sathiparan et al. 2006), cyclic (Mayorca and Meguro 2003), and dynamic loading. One-quarter scale models tested on a shake table have been studied (Meguro et al. 2005). In this study, in order to understand the dynamic response of masonry houses with and without PP-band mesh retrofitting, four more scale model shake table tests were carried out and the crack patterns, failure modes, and the overall effectiveness of the retrofitting technique were considered. This experimental program used one-quarter scale models of box-shaped structures with wooden truss roofs. In addition, the effect of adding surface plaster on top of the PP-bands was also studied.

Assuming that the houses in need of retrofitting have two rooms of 72×27 m^2 (Figure 3), a retrofit using around 4,500 to 5,000 m of PP-band would cost approximately 30 USD in the Kashmir region, for example. The total cost of retrofitting depends on how much of the work done is by the house owner and how much is contracted. A cost comparison with other retrofitting materials is shown in Table 1.

An automatic manufacturing process for PP-band mesh has not yet been developed. To prepare PP-band mesh, a portable plastic welder is a necessary tool. In order to prepare the mesh, each intersection has to be welded, one by one. A plastic welder can produce an ultrasonic wave that welds plastic materials quickly, as shown in Figure 4.

Figure 3. House in Pakistan retrofitted with PP-band mesh (JBIC 2007).

DESIGNING AND CONSTRUCTING THE MODELS

DESIGN OF THE MODELS

The dimensions and capacity of the shake table used for the tests limited the design of the model dimensions. The steel platform measured 1.5×1.5 m^2 in plan, and could carry a maximum payload of 2,000 kg. It was capable of operating at frequencies ranging from 0.1 to 50 Hz. The maximum acceleration input, under zero payload, was ± 2.0 g in the longitudinal direction and the maximum displacement was ± 100 mm. Considering the size and allowable loading conditions of the shake table, a one-quarter model scaling factor was adopted, as shown in Figure 5.

Four models of simple buildings were constructed following the rules of true replica modeling. This means that not only the dimensions but also the material properties were scaled. The dimensions of all four building models were $933 \times 933 \times 720$ mm, with 50 mm-thick walls. The size of the doors and windows was 243×485 mm and 325×245 mm, respectively, and these were set in opposite walls. The mortar thickness between adjacent brick layers was 5 mm. A wooden truss roof was used, above which, two 10 mm-thick inclined timber plates with dimensions of 1,033 mm $\times$ 600 mm were attached.

MODEL TYPE AND MATERIAL PROPERTIES

Of the four models, the first model, called A-NR-X, represented a box-type one-story building with a timber roof; the second model, called A-RE-X, represented a box-type one-story building with a timber roof that had been retrofitted using PP-band mesh; and the other two models, A-NR-P and A-RE-P, were similar to the first two models except that a surface finish covering the inside and outside of the walls had been applied.

Table 1. Comparison of masonry reinforcement material prices

Mesh type	Mesh cost (US$/m^2)
Welded wire steel mesh	1.95
Polymer mesh (Tensar BX1100)	2.00
Protection mesh	0.50
PP-band mesh	0.20

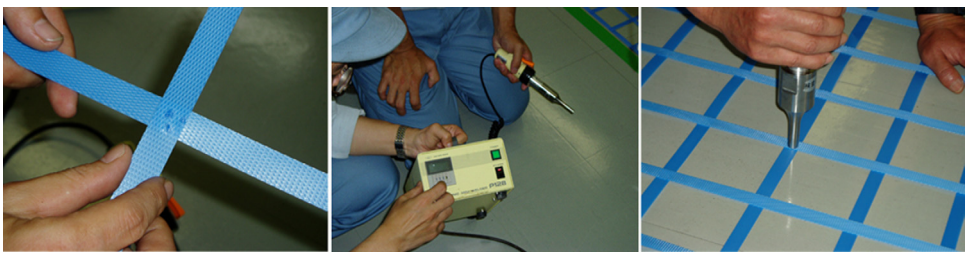

Figure 4. Manufacturing PP-band mesh.

As mentioned earlier, the main target of retrofitting with PP-band mesh is to improve the earthquake-safety of seismically vulnerable masonry houses in developing countries, so it was desirable to use materials with similarly low-strength characteristics in the tests. Because only strong bricks were available due to logistical issues, a very weak mortar mix was used in order to obtain low-strength masonry. The masonry brick units were a mixture of Mikawa clay (30%), ceramic waste soil (55%), sand (8%), and ceramic waste (7%) and the mortar was a mixture of river sand, Portland cement, lime, and water. To replicate the seismically vulnerable buildings targeted in this study we used unburnt bricks (adobe) and a cement, lime, and sand mixture with a 1:2.8:8.5 ratio as the mortar. The cement-to-water ratio was 33%.

The layout of specimens used for the direct compression, direct shear, and bond tests is shown in Figure 6. The material properties of each model were satisfactorily measured and can be seen in Table 2.

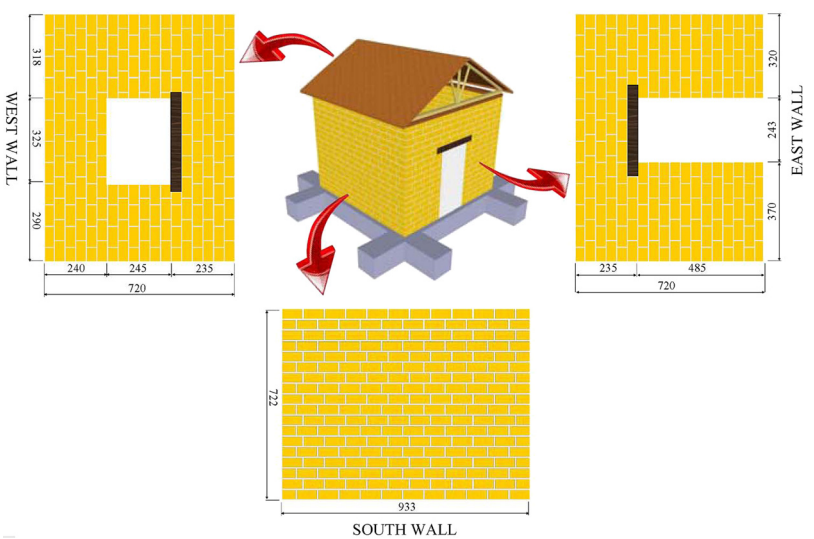

Figure 5. House model for shake table tests (dimensions in mm).

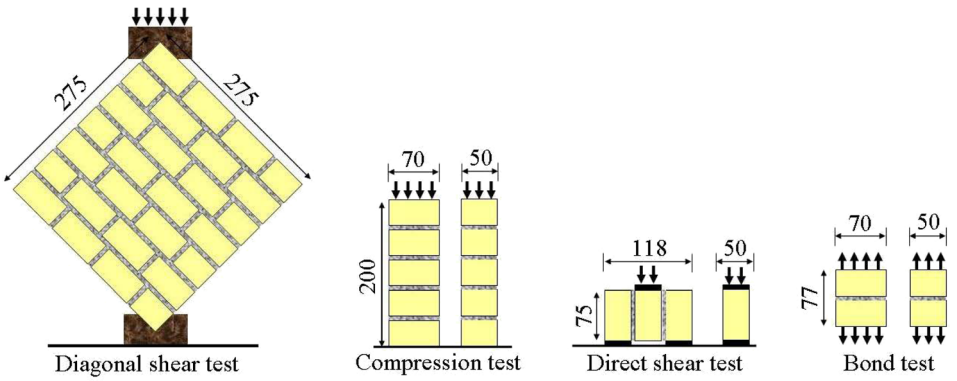

Figure 6. Layout of specimens used for material testing (unit: mm).

Preliminary testing of the PP-bands was carried out to check their deformational properties and strength. To determine the modulus of elasticity and ultimate strain, three bands were tested using a uniaxial tensile test. The bands were fixed at one end and an axial tensile force was applied to the other end. The initial distance between the two ends was 150 mm. The test was carried out under displacement control. The results are shown in Figure 7.

To calculate the stress in the bands, their nominal cross section, $15.5 \times 0.6\text{mm}^2$, was used. The thickness of the bands was not uniform due to surface corrugation. The tensile strength as well as the modulus of elasticity is summarized in Table 3.

All the bands exhibited a large deformation capacity, with more than 13% axial strain. The stress-strain curve is fairly bilinear, with an initial and residual modulus of elasticity of 3.19 GPa and 1.0 GPa, respectively. Given its large deformation capacity, it was expected that the PP-band mesh would improve the ductility of the retrofitted structures.

The efficiency of the PP-band mesh orientation on the masonry structures was tested under two conditions (Sathiparan et al. 2005): in Orientation 1 the PP-band mesh was oriented parallel to the masonry joints, while in Orientation 2 the PP-band mesh was oriented at a 45° angle in relation to them. Although Orientation 1 did not utilize the full capacity of the mesh, it did improve the seismic behavior of the wall to a degree, which can be

Table 2. Material properties of the models

					Mechanical properties (in MPa)			
Model no.	Model name	Roof condition	Retrofitted condition	Surface finish	Diagonal shear strength	Compression strength	Shear strength	Bond Strength
1	A-NR-X	√			0.041	4.28	0.0057	0.0046
2	A-RE-X	√	√		0.045	4.36	0.0068	0.0046
3	A-NR-P	√		√	0.048	4.29	0.0061	0.0050
4	A-RE-P	√	√	√	0.050	4.35	0.0056	0.0048

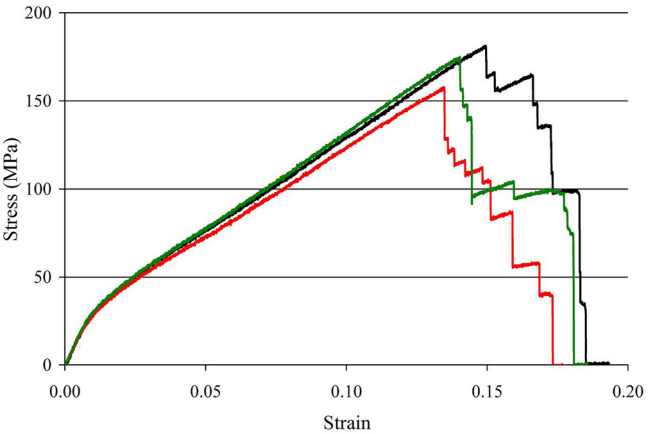

Figure 7. Behavior of PP-bands under tension loading.

considered enough for earthquake damage mitigation. In addition, Orientation 1 is easier to install, so it was selected as the best solution for retrofitting.

MAKING THE MODELS

The specimens consisted of 18 rows of 44 bricks in each layer, except at the openings. It took two days to construct one specimen. The first 11 rows were constructed on the first day and the remaining rows were done the following day. The geometry, construction materials and mixture proportion, construction process and technique, and the other conditions that could have affected the strength of the building models were kept identical.

The preparation of the models is explained below and is illustrated in Figure 8:

- The PP-bands were arranged in a mesh pattern and connected at the intersections using a portable plastic welder.
- The structure walls were cleaned and any loose pieces of brick were removed.
- Straw, which had been placed in the holes to be used for securing the mesh, was removed. (In this experiment, during construction of the model houses, straw was used to create holes approximately every 160 mm along the walls. In the case of existing structures, holes can be prepared by drilling through the wall.)

Table 3. Results of the axial tension test on PP-bands

Specimen	Maximum tensile stress (MPa)	Initial modulus of elasticity (GPa)	Residual modulus of elasticity (GPa)
PP- 1	181.21	3.18	1.07
PP- 2	157.74	3.07	1.02
PP- 3	174.71	3.32	1.09
Average	171.22	3.19	1.06

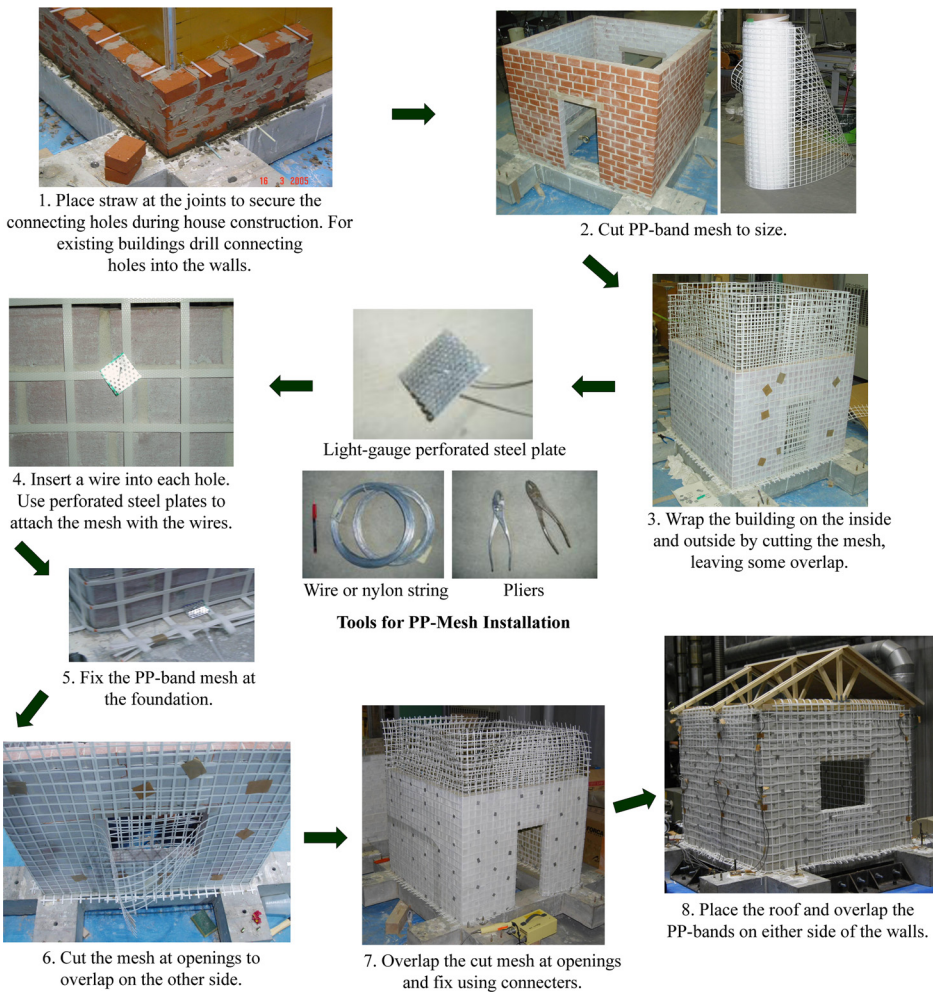

Figure 8. PP-band mesh retrofitting procedure for masonry houses.

- The corners of the walls and their edges were wrapped in mesh. The overlapping length was left long enough to accommodate wire connectors, as this was the only system used to connect the mesh to the structure.
- Wires were passed through the holes in the wall and were used to connect the mesh on both the inside and outside of the structure. In order to prevent the wires from cutting the mesh, a piece of plastic—or any other stiff material—can be placed between the mesh and the wire. The wire connectors should be as close as possible to the wall intersections and corners.
- The top and bottom edges of the mesh were connected with steel wires. The bottom edge should be connected to the structure foundation as securely as possible. When installing PP-band mesh on existing houses, it could be hard to excavate the ground to bury the mesh and affix it to the foundation of the house. Simply securing the

mesh above ground will save on operational costs as well as workload. Similarly, for existing houses, the top edges of the PP-band mesh need not be wrapped at the roof level.

- Wire connectors were fixed around the openings after the mesh was cut and folded over onto the other side of the walls.

The scale models were wrapped with mesh made of PP-bands that were 6 mm wide by 0.32 mm thick, and that intersected every 40 mm in a grid pattern. The distance between the wire connectors was 160 mm, equivalent to four times the length between the mesh intersections. In other words, there were 36 connectors per square meter. When two pieces of mesh overlapped, they were attached with two rows of wire connectors (at least 200 mm).

TEST PROCEDURE

INPUT MOTION

Tests were carried out in a series on the shake table at the Institute of Industrial Science, University of Tokyo. Simple and easy-to-use sinusoidal motions of frequencies ranging from 2 to 35 Hz and amplitudes ranging from 0.05 to 1.4 g were applied to the specimens to obtain the dynamic response of both the retrofitted and unretrofitted structures. This simple input motion was applied because of its adequacy for later use in the numerical modeling. Figure 9 shows the typical shape of the applied sinusoidal wave input motion.

Loading was started with a sweep motion with an amplitude of 0.05 g for all frequencies from 2 to 50 Hz in order to identify the dynamic properties of the models. The numbers in Table 4 indicate the run numbers. The general trend of loading was from higher frequencies to lower frequencies and from lower amplitudes to higher amplitudes. Higher-frequency motions were skipped toward the end of the runs.

MEASUREMENT OF DYNAMIC CHARACTERISTICS

The test specimens were fixed on a shake table measuring 1.5 × 1.5 m. The shake table system at the University of Tokyo is capable of controlling six degrees of freedom and

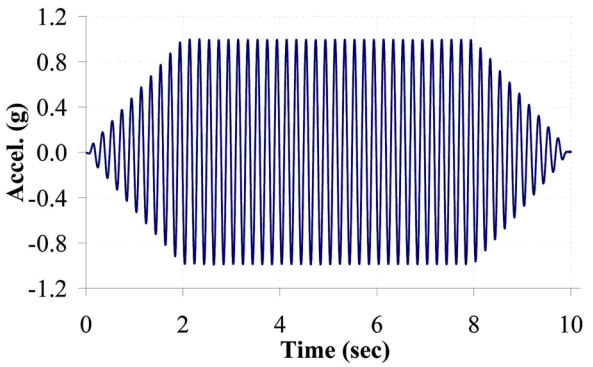

Figure 9. Typical shape of the applied sinusoidal wave.

Table 4. Loading sequence

	Frequency							
Amplitude	2 Hz	5 Hz	10 Hz	15 Hz	20 Hz	25 Hz	30 Hz	35 Hz
1.4 g		50						
1.2 g	54	49						
1.0 g		48						
0.8 g	53	47	43	40	37	34	31	28
0.6 g	52	45	42	39	36	33	30	27
0.4 g	51	44	41	38	35	32	29	26
0.2 g	46	25	24	23	22	21	20	19
0.1 g	18	17	16	15	14	13	12	11
0.05 g	10	09	08	07	06	05	04	03
sweep					01, 02			

operating at frequencies ranging from 0.1 to 50 Hz. It has a maximum displacement of ±100 mm and it can handle specimens with a maximum weight of 2 tons. In this experiment, the shake table system was limited to one direction of shaking for simplicity.

In each model, 24 accelerometers, 18 on the walls and 6 on the roof, were installed to assess the global and local behavior of the specimens, as shown in Figure 10. The number of accelerometers was 13, 7, and 4 in the direction of shaking, the transverse direction, and the vertical direction, respectively.

Five lasers, in the N–S direction, were used to measure displacements. Lasers L1, L2, and L3 obtained measurements of the wall deformation at the top of the model walls in the direction of shaking. Laser L4 recorded the wall deformation at the center. Laser L5 recorded the deformation at the base. The measured data were recorded continuously throughout the tests. The sampling rate was 1/500 sec. in the all runs.

Table 5 shows the natural frequency of each model.

SHAKE TABLE TESTS

Models A-NR-X and A-RE-X

In both specimens, due to shrinkage, some minor cracks were observed before the testing. These cracks mainly appeared close to the openings, in the horizontal direction. For both specimens, up to Run 20, no major cracking was observed. Major cracks were observed close to the openings starting at Run 21. Figure 11 shows the crack patterns for A-NR-X and A-RE-X after Run 39. At this level of shaking the lateral drift was 1.21 mm and 1.31 mm for models A-NR-X and A-RE-X, respectively. Up to this point, the crack patterns in both specimens looked similar, although the damage to A-RE-X seemed slightly more severe on the eastern wall. But in general, the sequence of the appearance of cracks was the same in both models. At first, inclined cracks appeared that began at the corner of the openings on the west wall, where the window was located, and reached the top and

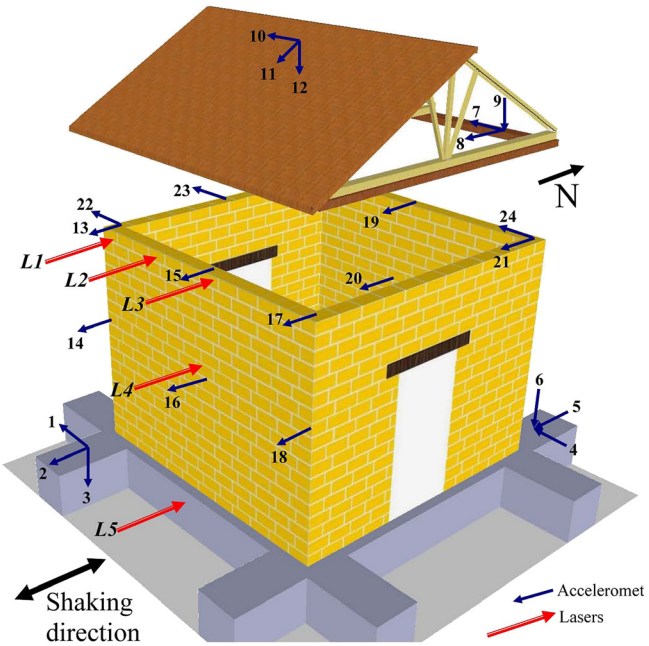

Figure 10. Accelerometers and laser position (arrows indicate the measured positive direction).

bottom of the model. In the east wall, where the door was located, the inclined cracks were accompanied by horizontal cracks that reached the north and south walls. In the case of A-NR-X, an additional horizontal flexural crack on the top layer of the north and south walls was observed.

Although the cracks widened with each successive run after Run 39, Run 44, which corresponded to a lateral drift of 6.92 mm, was critical. Figure 12 shows the crack patterns for A-NR-X and A-RE-X after run 44. There were many cracks observed in the walls in the direction of shaking. These became wider at higher excitations and as the connections between adjacent walls become weaker. At the end of Run 44, as shown in Figure 13, the portion of the wall above the door lintel separated totally from the model. During Run 45, the entire top portion of the wall separated from the specimen and collapsed. At this point, the roof was supported by only two walls, which were in the direction of shaking. Due to the out-of-plane load, the walls burst outward in the direction of shaking. This finally led to

Table 5. Initial natural frequency of each model

Model	Natural frequency
A-NR-X	38.0
A-RE-X	40.3
A-NR-P	40.2
A-RE-P	40.2

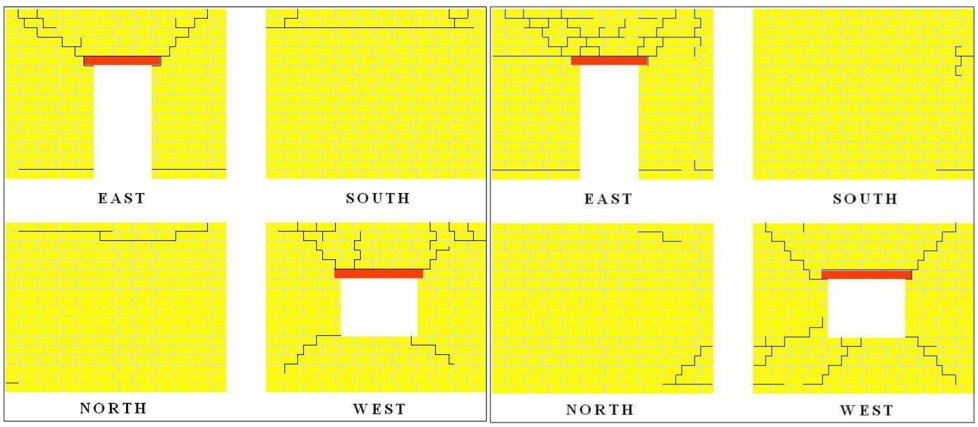

(a) (b)

Figure 11. Crack patterns of models (a) A-NR-X and (b) A-RE-X after Run 39.

the collapse of the structure. Run 45 corresponded to a base velocity and displacement of 187 mm/s and 6 mm, respectively.

In the case of A-RE-X, each successive run after Run 39 caused new cracks. The cracks widened and sliding along the mortar joints could be clearly observed. This was true especially in the north and south walls, which were subjected to out-of-plane loads and were extensively cracked, causing large deformations during the shaking. At the final stage of the test, during Run 52, during which the model had a lateral drift of 28.90 mm, virtually all the brick joints were cracked and the model had substantial permanent deformations. This input motion corresponded to a velocity and displacement of 467.5 mm/s and 37.3 mm, respectively, two and a half times larger than the velocity and six times larger than the

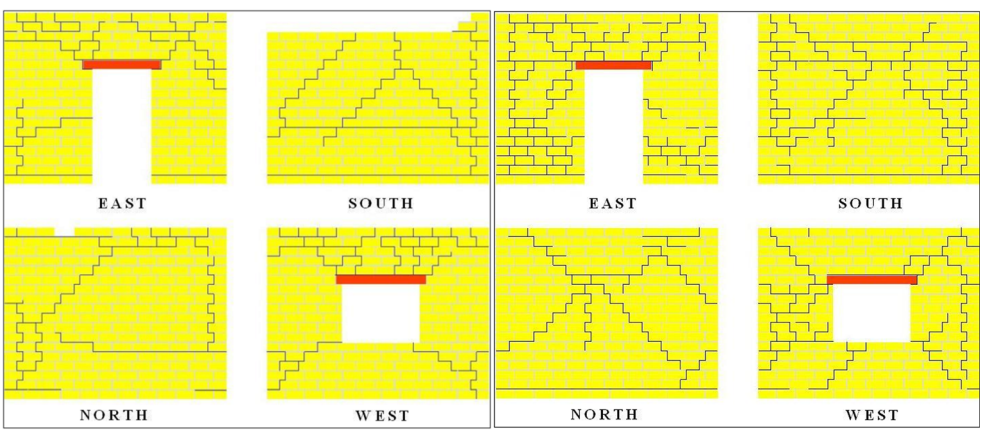

(a) (b)

Figure 12. Crack patterns of models (a) A-NR-X and (b) A-RE-X after Run 44.

(a) (b)

Figure 13. Partial collapse of (a) the unretrofitted model, A-NR-X and (b) the retrofitted model, A-RE-X after Run 44.

displacement that caused the failure of A-NR-X. However, the building did not lose overall integrity and collapse was prevented.

As observed in previous experimental studies of masonry structures retrofitted with PP-bands (Sathiparan et al. 2005), the PP-band mesh had little effect on the structural behavior of the models before cracking occurred. This is because PP-band mesh is not very stiff as compared to the stiffness of the masonry structure.

Models A-NR-P and A-RE-P

In specimen A-NR-P, major cracks were observed close to the connection between the roof and the south wall at Run 26, and they widened with each successive run. At Run 43, during which the model had a lateral drift of 2.62 mm, a lot of damage was observed in model A-NR-P. Separation between the east wall and its adjacent walls was observed. Furthermore, a lot of the surface finish separated from the walls. At Run 44, the top corners of the east wall and the adjacent walls were totally separated from the specimen. At Run 45, the entire top part of the north and south walls totally separated from the specimen. At this point, the roof was supported by only two walls, which were perpendicular to the direction of shaking. The structure finally collapsed during Run 47. This input motion corresponded to a velocity and displacement of 250 mm/s and 8 mm, respectively. Figure 14 shows the unretrofitted and retrofitted house models at the end of Run 47.

In the case of the retrofitted model A-RE-P, up to Run 39, there were only a few cracks observed (Figure 15). After that, however, the cracks widened and the propagation of new cracks continued until Run 50. Although there were cracks throughout all the walls at the end of Run 50, the specimen did not lose stability. At this level of shaking the lateral drift was 24.3 mm. Some bricks from the bottom part of the east wall spilled out from beneath the PP-band mesh. Therefore, some looseness was observed in the bottom part of the wall. But even at this very high input motion, most of the surface finish was still attached to the walls. At the final stage of the test, Run 54, with a base displacement of 74.6 mm, 9 times more than the input displacement applied in Run 47, and 3.7 times more velocity, virtually

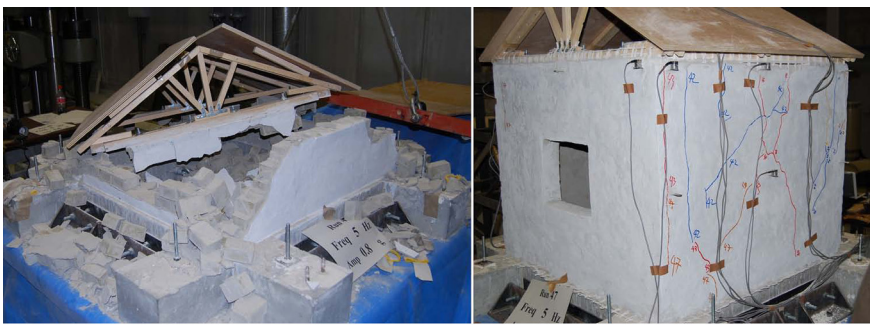

(a) (b)

Figure 14. (a) The unretrofitted model, A-NR-P, and (b) the retrofitted model, A-RE-P, after Run 47.

all the brick joints were cracked, and the building had substantial permanent deformations. However, the building did not lose overall integrity and collapse was prevented. Thus, the PP-band retrofitting technique maintained the integrity of the structural elements. Further, the retrofitted model showed better energy dissipation, as many new cracks were propagated without losing the overall integrity and stability of the structure.

The retrofitted model with the layer of surface finish showed a better bond between the finish and the walls than did the model that hadn't been retrofitted, as shown in Figure 16.

The PP-band mesh effectively distributed the cracks in the retrofitted models, whereas in the unretrofitted models, after a limited number of cracks the structure was sectioned into several pieces that shook independently and interacted with one another. The only stabilizing mechanism preventing toppling was the weight of each piece. There was no possibility of transferring and distributing stresses to the undamaged portions of the structure. In the case of

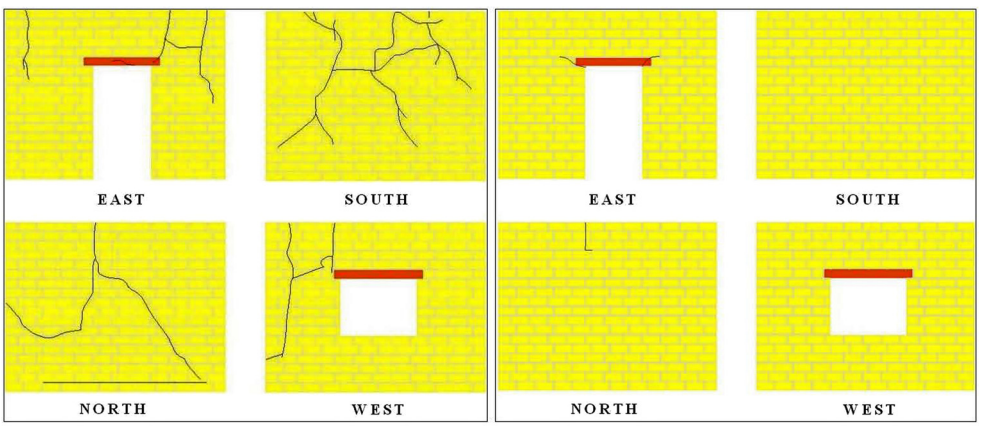

(a) (b)

Figure 15. Crack patterns of models (a) A-NR-P and (b) A-RE-P after Run 39.

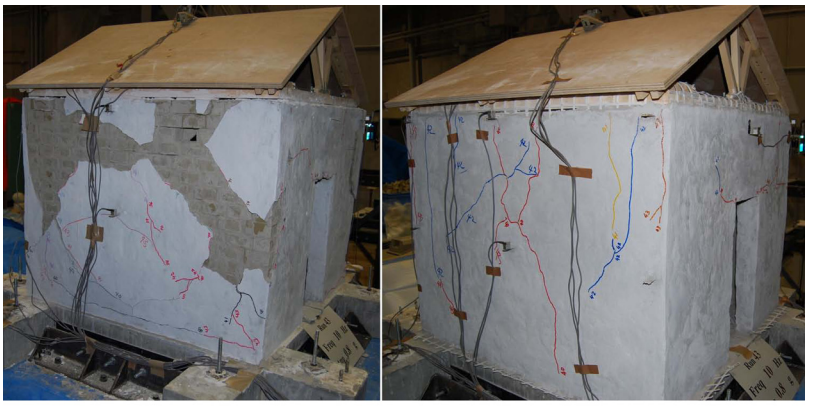

(a) (b)

Figure 16. (a) The unretrofitted model, A-NR-P, and (b) the retrofitted model, A-RE-P, after Run 43.

the retrofitted structures, the damage was similar to that in the unretrofitted models in the initial loading stages, but at later stages the PP-band mesh distributed the stress through the cracks, transferring it to the undamaged portions of the structure. As a result, new cracks appeared. The PP-band mesh also effectively stabilized the structure and prevented wall collapse. Furthermore, it controlled the corner damage experienced by the structure, which is one of the common failure mechanisms in unreinforced masonry buildings.

In addition, the effectiveness of the retrofit is highly dependent on how tightly the mesh is attached to the structure. The tighter the mesh is attached, the earlier its effects will be observed (Sathiparan et al. 2008). This observation shows the importance of covering the mesh with mortar in order to fill any gaps between the mesh and the masonry and to improve the confining effect of the PP-band mesh, thus improving the structural performance of the building. In addition, mortar also protects the mesh against UV radiation and severe temperature variations, and it provides a smooth finish for the retrofitted structure.

ANALYSIS OF THE TEST RESULTS

In order to analyze the test results, the Japan Meteorological Agency (JMA) intensity and Arias intensity of the input motion as a function of time was calculated.

PERFOMANCE EVALUATION BASED ON JMA SCALE

The JMA seismic intensity scale is a measure used in Japan to indicate the strength of earthquakes. Unlike the Richter scale (which measures the total magnitude of the earthquake, and represents the size of the earthquake with a single number) the JMA scale describes the degree of shaking at a point on the Earth's surface.

The performance of the models was assessed based on the damage level of the buildings at different levels of shaking. The performance was evaluated using a five-level scale based on the European Macroseismic Scale, EMS-98 (Grünthal 2001): light structural damage,

Table 6. Damage categories

Category	Damage extension
D0: No damage	No damage to structure
D1: Light structural damage	Hairline cracks in very few walls. The structural resistance capacity did not decrease noticeably.
D2: Moderate structural damage	Small cracks were observed on masonry walls. The structure resistance capacity decreased partially.
D3: Heavy structural damage	Large, deep cracks were observed on masonry walls. Some bricks had fallen. There was failure in the connection between two walls.
D4: Partial collapse	Serious failure and partial structural failure was observed on walls and roofs, respectively. The building was in a dangerous condition.
D5: Collapse	Structure was totally or partially collapsed.

moderate structural damage, heavy structural damage, partial collapse, and collapse, as shown in Table 6.

Figure 17 shows the damage evaluation for all models. In the case of the house models without a surface finish, until Run 26 both models showed light structural damage. At this point, model A-NR-X developed moderate damage until Run 40. After that it showed rapid degradation and then partially collapsed after Run 44. This input motion corresponded to a JMA intensity of 5-.

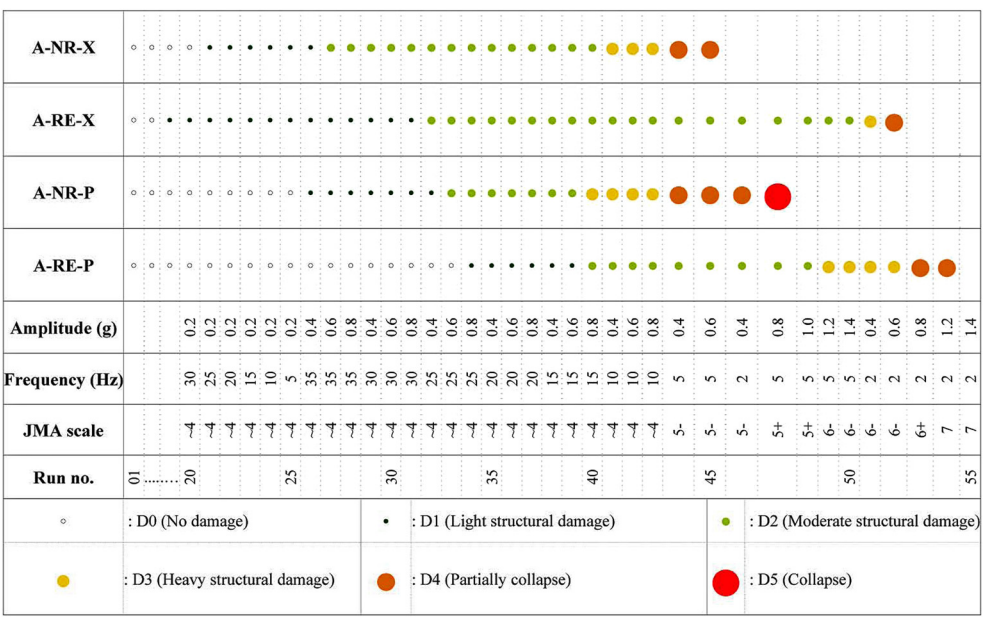

Figure 17. Performance evaluation based on the JMA scale.

The damage to model A-RE-X, on the other hand, progressed more gradually. Although the structure was subjected to four runs with and intensity of JMA 6-, it did not collapse. The specimen cracked, but no permanent deformations were observed and partial collapse didn't happen until Run 50. In the field, a structure with this degree of damage can be readily repaired and used. Figure 18 (right) shows A-RE-X after Run 52, which corresponded to a JMA intensity of 6+. Even at this stage, the permanent deformations suffered by the structure were limited. Furthermore, escape routes such as doors and windows were secured.

In the case of the house models with a surface finish (A-NR-P and A-RE-P), total collapse of the unretrofitted building occurred at the 47th run, at an intensity of JMA 5+. The retrofitted building suffered moderate structural damage at Run 47, the same run during which the unretrofitted building totally collapsed. Moreover, the retrofitted building maintained a level of moderate structural damage through Run 48, which corresponded to an intensity of JMA 5+. It should be noted again that this model survived seven more runs, many of which were at intensities higher than JMA 5+, which was the maximum intensity withstood by the unretrofitted building before collapse.

It can be concluded that a structure retrofitted with PP-band mesh would be able to resist strong aftershocks. Moreover, this study proves that even though a house retrofitted with PP-bands may crack after a strong earthquake, it can be repaired and can be expected to withstand subsequent strong shaking.

PERFORMANCE EVALUATION BASED ON ARIAS INTENSITY

The Arias intensity was initially defined as (Arias and Hansen 1970):

$$I_a = \frac{\pi}{2g}\int_0^t a^2(t)dt \tag{1}$$

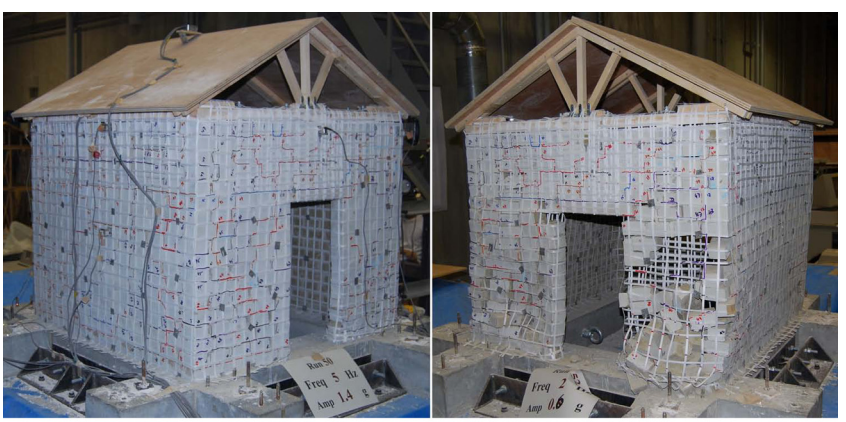

(a) (b)

Figure 18. Retrofitted model, A-RE-X, after (a) Run 50 and (b) Run 52.

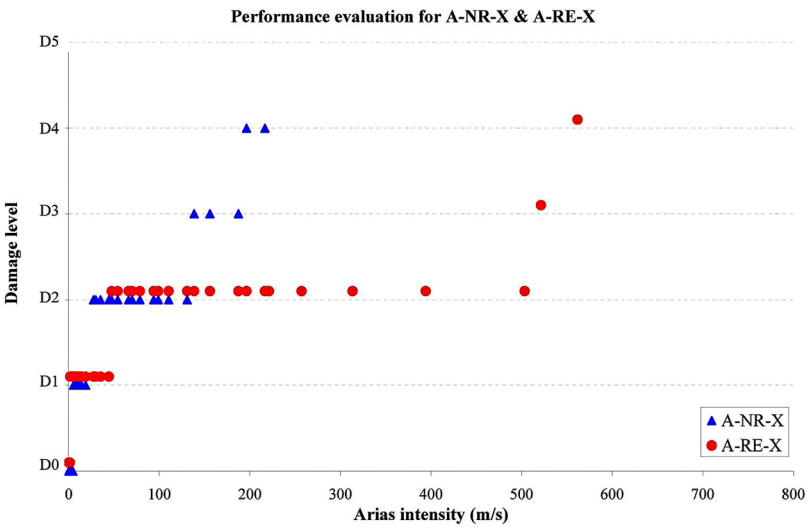

Figure 19. Performance evaluation based on Arias intensity for models A-NR-X and A-RE-X.

and was called scalar intensity. It is directly quantifiable through the acceleration record a*(t)*, integrating it over the total duration of the earthquake. The Arias intensity is claimed to be a measure of the total seismic energy absorbed by the ground. It gives the cumulative effect of seismic input motions.

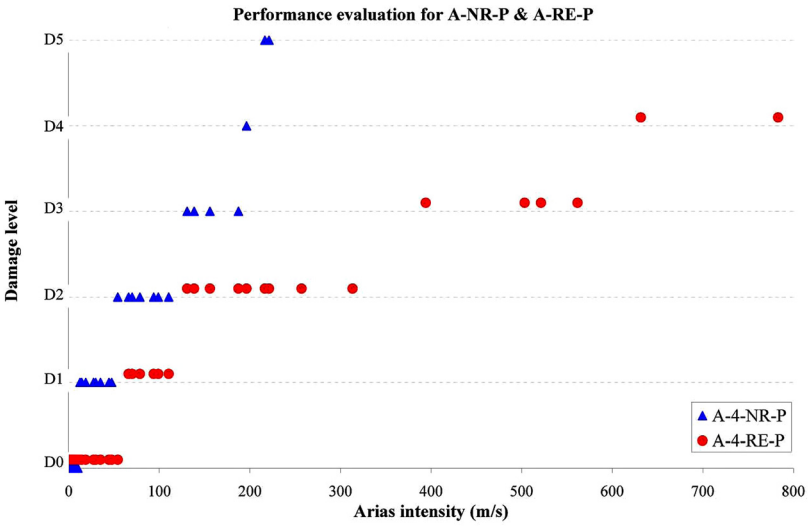

Figure 20. Performance evaluation based on Arias intensity for models A-NR-P and A-RE-P.

Table 7. Drift levels (in mm) at various damage levels

	Damage level		
Model name	Light structural damage	Moderate structural damage	Heavy structural damage
A-NR-X	~0.02	0.02–0.20	0.20–0.47
A-RE-X	~0.03	0.03–0.97	0.97–4.01
A-NR-P	~0.02	0.02–0.08	0.08–0.36
A-RE-P	~0.13	0.13–2.48	2.48–6.93

Figures 19 and 20 show the performance level of each specimen against the dynamic motion. From the results, it can be seen that the retrofitted model performed at least three times better than the unretrofitted model.

LATERAL DRIFT

In design, drift (i.e., story drift/story height) limits can be used to control the extent of structural and nonstructural damage to a building. Hence the drift levels that correspond to the onset of major damage in the test models are summarized in Table 7. These can be used as approximate guidelines for design.

As can be observed from Table 7, in all the models tested, moderate structural damage occurred at a drift ratio between 0.02% and 0.03%, except in A-RE-P. For both unretrofitted models, very heavy structural damage and partial collapse occurred at a drift of around 0.4%. However, in the retrofitted models, heavy structural damage and partial collapse occurred at a drift of 4% for A-RE-X and 6.9% for A-RE-P. These figures indicate that a retrofitted house could withstand a lateral drift level at least ten times higher than an unretrofitted house, even without any surface finish.

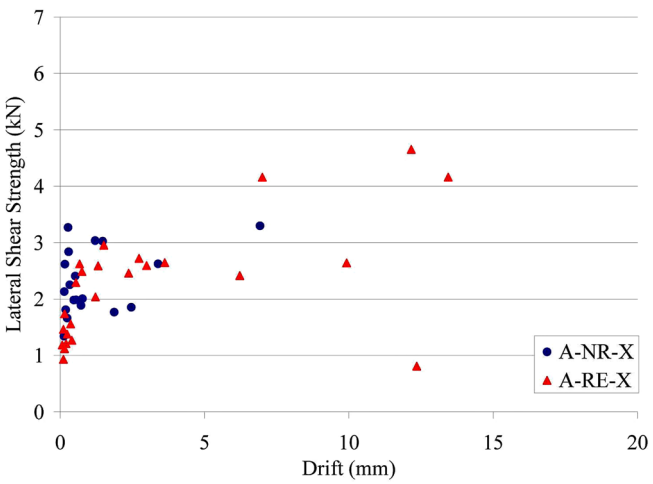

Figure 21. Comparison of lateral shear force between A-NR-X and A-RE-X.

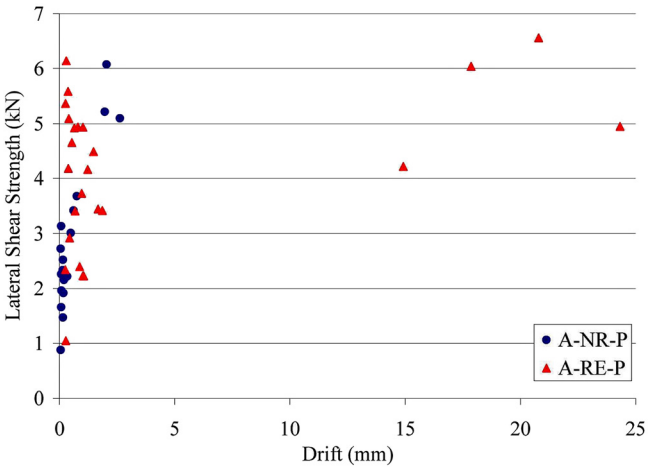

Figure 22. Comparison of lateral shear force between A-NR-P and A-RE-P.

Considering the predominant shape of the first mode of vibration, assuming that the observed mode shape is stable during shaking, and neglecting damping, base shear, and story height, lateral force can be determined. Lateral shear force is determined as a sum of the inertial forces acting on walls:

$$SS = \sum_{1}^{n} m_i a_i \tag{2}$$

Where SS is the lateral shear force, m_i is the pertinent mass at each location, a_i is the acceleration, and n is the number of locations considered for the calculation. Figure 21 shows the lateral shear force variation with lateral drift for the models without any surface finish and for the models with surface finish, respectively. In both cases, before major cracking occurred, there was no difference in lateral shear force between the unretrofitted and retrofitted models.

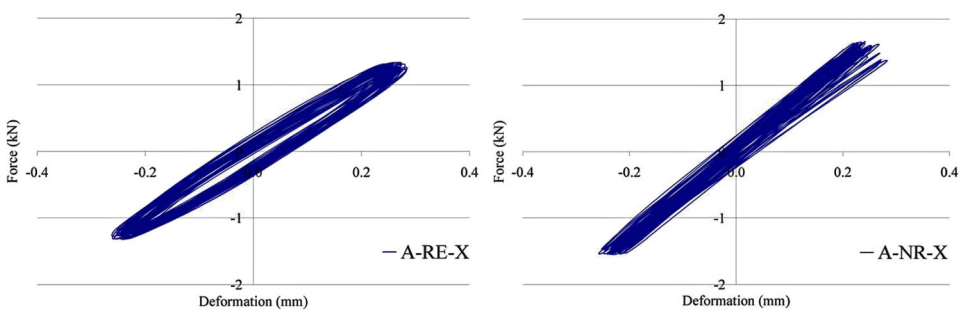

Figure 23. Lateral force-deflection hysteresis loops for Run 32.

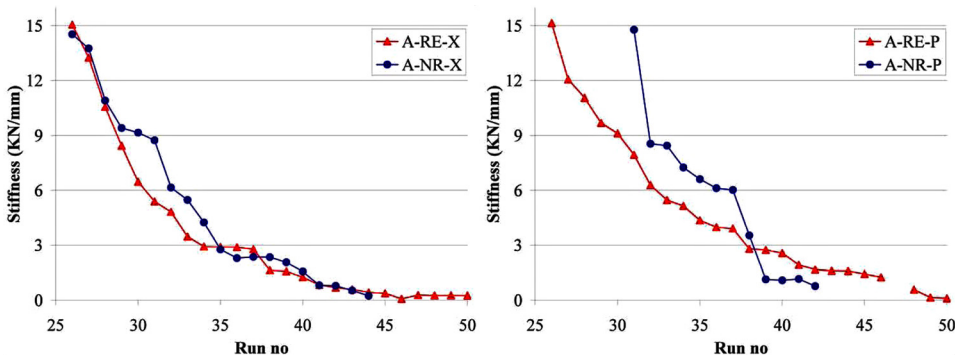

Figure 24. Stiffness degradation for each house model.

However, after cracking, both retrofitted specimens withstood higher lateral forces—up to more than 20 mm of lateral drift. These results indicate that after cracking, PP-band mesh positively influences the lateral resistance of buildings.

STIFFNESS DEGRADATION

Masonry is an inelastic structural material that doesn't behave elastically, even in the range of small deformations. However, for practical reasons, the effective stiffness of a wall, defined as the slopes of the hysteresis curve (such as the graph shown in Figure 23), is determined from the ratio between lateral force and deformation in a house model. The stiffness degradation values calculated after each run are shown in Figure 24.

ENERGY DISSIPATION

The comparison of the values of energy related to different levels of base excitation is meaningful (Benedetti et al. 2001). However, in some instances it is useful to normalize the cumulated energy time histories with respect to the impedance of the excitation. The energy

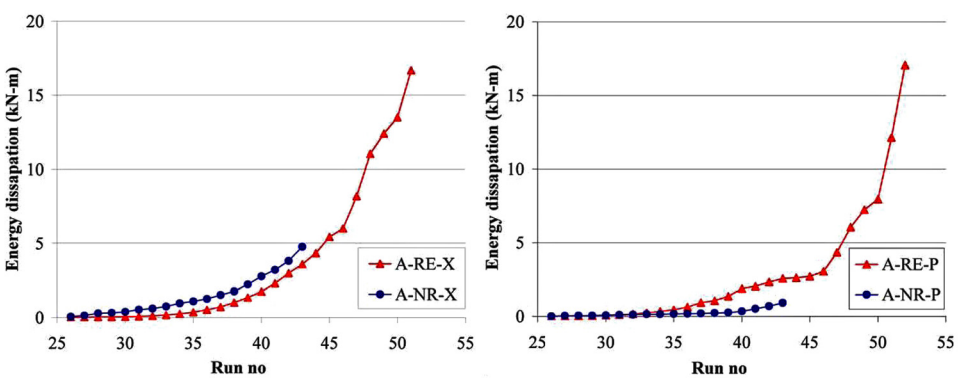

Figure 25. Energy dissipation for each house model.

dissipated in each cycle is the area enclosed by the hysteresis loop corresponding to that cycle. The energy dissipated by the whole house model corresponds to the total force and the horizontal displacement at the top of the house model.

To assess the overall performance of the structures, energy dissipation in terms of input runs is shown in Figure 25. Generally, the energy dissipation capacity of the retrofitted house specimens was much larger than that of the unretrofitted house specimens.

CONCLUSIONS

Past earthquakes have shown that the collapse of seismically vulnerable masonry structures is responsible for most of the earthquake fatalities in developing countries. Thus, it is crucial to improve their seismic performance in order to reduce future fatalities and to protect the existing housing stock. To encourage seismic retrofitting, inexpensive and easy-to-implement technical solutions are desirable. Retrofitting using PP-band mesh satisfies these requirements.

Shake table experiments showed that scaled dwelling models with PP-band mesh retrofitting can withstand larger and more repetitive shaking than those without PP-band retrofitting. When a surface finish was applied to the retrofitted house model there was an improved bond between the PP-band mesh and the brick walls and the surface plaster remained more securely attached to the wall during shaking. This improved bond was not observed in the unretrofitted model. In addition to this, covering the mesh with mortar fills any gaps between the mesh and masonry, thus improving the structural performance of the building. The mortar also protects the mesh against UV radiation and severe temperature variations, as well as providing a smooth finish on the retrofitted structure.

The experimental results showed that this retrofitting technique can enhance the safety of both existing and new masonry buildings, even in a worst-case-scenario earthquake with ground motion intensities measuring JMA 7. Therefore, PP-band retrofitting is an optimum solution for promoting safer building construction in developing countries and can contribute to earthquake disaster mitigation in the future.

REFERENCES

Arias, A., and Hansen, R. J., 1970. A measure of earthquake intensity, in *Seismic Design for Nuclear Power Plants*, MIT Press, Cambridge, MA, 438–483.

Benedetti, D., Carydis, P., Pezzoli, P., 2001. Evaluation of the seismic response of masonry buildings based on energy functions, *Earthquake Engineering and Structural Dynamics* **30**, 1061–1081.

Coburn, A., and Spence, R., 2002. *Earthquake Protection*, 2nd edition, John Wiley & Sons, Ltd, Chichester, UK, 420 pp.

Grünthal, G. (ed.), 2001. *European Macroseismic Scale 1998 (EMS-98)*, Centre Europèen de Géodynamique et de Séismologie, Luxembourg.

Mayorca, P., and Meguro, K., 2003. Efficiency of polypropylene bands for the strengthening of masonry structures in developing countries, in *Proc. of the 5th International Summer Symposium*, CD-ROM, Japan Society of Civil Engineers, Tokyo, Japan.

Mayorca, P., and Meguro, K., 2004. An innovative seismic strengthening method for unreinforced masonry structures using pp-band mesh, *Third International Symposium on New Technologies for the Urban Safety of Mega Cities in Asia*, October 2004, Agra, India.

Mayorca, P., 2001. Buildings and dwellings in the January 13, 2001 Off the Coast of El Salvador Earthquake, Earthquake Engineering Committee, CD-ROM, Japan Society of Civil Engineers, Tokyo, Japan.

Meguro, K., Ohi, K., Mayorca, P., and Guzmán, R., 2001. *Damage to Buildings and Dwellings, Provisional Report on the June 23, 2001 Atico Earthquake*, Japan-Peru Joint Reconnaissance Team and Japan Society of Civil Engineers, Tokyo, Japan.

Meguro, K., Mayorca, P., Sathiparan, N., Guragain, R., and Nesheli, N., 2005. Shaking table tests of 1/4 scaled masonry models retrofitted with PP-band meshes, in *Proc. of the Fourth International Symposium on New Technologies for the Urban Safety of Mega Cities in Asia*, Nanyang Technological University, Singapore, 9–18.

Japan Bank for International Cooperation (JBIC), 2007. *Pilot Studies for Knowledge Assistance for Verification and Promotion on a New Seismic Retrofitting Method for Existing Masonry Houses by Polypropylene Band Mesh (The Islamic Republic of IRAN)*, International Center for Urban Safety Engineering, and OYO International Corporation, Tokyo, Japan

Sathiparan, N., Mayorca, P., Nesheli, K., Ramesh, G., and Meguro, K., 2005. Experimental study on in-plane and out-of-plane behavior of masonry wallettes retrofitted by PP-band meshes, *Seisan Kenkyu Bimonthly Journal of Institute of Industrial Science* **57**, 530–533.

Sathiparan, N., Mayorca, P., Nesheli, K., Ramesh, G., and Meguro, K., 2006. Experimental study on unburned brick masonry wallettes retrofitted by PP-band meshes, *Seisan Kenkyu Bimonthly Journal of Institute of Industrial Science* **58**, 301–304.

Sathiparan, N., Mayorca, P., and Meguro, K., 2008. Parametric study on diagonal shear and out-of-plane behavior of masonry wallettes retrofitted by PP-band mesh, *14th World Conference on Earthquake Engineering*, 12–17 October 2008, Beijing, China.

Yoshimura, M., and Meguro, K., 2004. Proposal of retrofitting promotion system for low earthquake-resistant structures in earthquake prone countries, *13th World Conference on Earthquake Engineering*, 1–6 August 2004, Vancouver, Canada.

(Received 8 December 2009; accepted 21 February 2011)